Journal of Applied Fluid Mechanics, Vol. 16, No. 7, pp. 1331-1344, 2023.
Available online at www.jafmonline.net, ISSN 1735-3572, EISSN 1735-3645.
https://doi.org/10.47176/jafm.16.07.1706

Studies on the Extraction of the Guaranteed Fuel Reserve in the Tanks of the Expended Stage

B. Akylbek [1,2†], Y. Gulnaz [1,2], T. Valery [4], K. Maksat[2] and S. Nurlan [3]

[1] *al-Farabi Kazakh National University, Almaty, 050040, Kazakhstan*
[2] *Institute of information and computational technologies, Almaty, 050000, Kazakhstan*
[3] *Almaty University of Power Engineering and Telecommunication, Almaty, 050013, Kazakhstan*
4 Omsk State Technical University, Omsk, 644050, Russia

†*Corresponding Author Email: a.bapyshev@aues.kz*

(Received December 13, 2022; accepted March 9, 2023)

ABSTRACT

The hard landing of the spent stage of promising launch vehicles (LV) in the designated areas of the fall leads to the collapse of the structure, the spillage of the remnants of the guaranteed fuel reserve, the outbreak of fires, and, as a result, require large expenditures for the complete elimination of man-made consequences. Residues of the guaranteed fuel are additional stocks of propellant components in the rocket blocks of the stage of LV, designed to compensate for the disturbing factors acting in flight on the LV. They are characterized by carcinogenic and mutagenic effects on the environment. The article considers the issue of extraction of unprocessed residues of guaranteed fuel. An experimental stand and a program for conducting experiments have been developed to study the extraction process. The purpose of the study is to conduct a comparative analysis of the results of mathematical modeling and physical modeling. Based on the results of the physical experiment, a mathematical model, and the results of a comparative study of two types of models are presented: The calculated heat carrier (HC) temperatures at the experimental model setup (EMS) inlet (according to the first law of thermodynamics and the Navier-Stokes equations) and the measured HC temperature at the EMS inlet during experiments were compared.

Keywords: Launch vehicle; Guaranteed fuel reserves; Liquid rocket engine; Gasification; Experimental stand; Heat carrier; Modeling.

NOMENCLATURE

ρ, p, T	density, pressure and temperature, respectively	T^*	steam temperature near the liquid in the container
λ	thermal conductivity	T_{sat}	saturation temperature of water at pressure in the container
S_h	the amount of heat including heat from chemical reactions, or other sources of heat	μ	flow coefficient
hj	particle enthalpy	F_{out}	the area of the passage section of the outlet hole
M	molar mass of the liquid	$p(t)$	pressure in the tank
R	gas constant	$T(t)$	temperature in the tank
ρ_l	density of the liquid phase	L	heat of vaporization

1. INTRODUCTION

The work (Shatrov *et al.* 2016) explains that some environmental problems of launch vehicles are associated with spent stages and the presence of a guaranteed fuel reserve (GFR) in their fuel tanks, which is determined by two components - a constant (residues of non-intake in fuel tanks and lines, engine refueling) and probabilistic (unused guaranteed reserves, excess refueling of working fuel with a mass of the output payload less than the calculated one, refueling error, errors in the operation of fuel consumption control systems, accuracy of rocket fuel component refueling systems, temperature spread, etc.).

The hard landing of the expended stages (ES) of the LV in the designated areas of the fall leads to the collapse of the structure, the spillage of the GFR residues, the occurrence of fires and, as a result,

requires large expenditures for the complete elimination of man-made consequences.

To eliminate the GFR residues after turning off the main liquid-propellant rocket engine (LPRE) on the expended booster of the first stage of the launch vehicle, technological, circuit and design solutions were implemented to discharge the residues of asymmetric dimethylhydrazine into the atmosphere through the combustion chamber of the main LPRE. This led to a redistribution toxic emission between the atmosphere and the impact area (IA), without solving the general task of reducing emissions of toxic GFR during the launch of the launch vehicle.

The existing developments to rescue the ES simultaneously provide for a number of tasks, the main of which is to increase the competitiveness of the corresponding class of launch vehicles due to the multiple use of the ES, while it becomes possible to simultaneously reduce the technogenic impact of launches of the launch vehicle and in the impact areas.

To solve the problem of ES rescue, rescue systems are used, implemented by various ballistic schemes of ES flight along the descent trajectory:

– rocket-dynamic maneuver (vertical landing) of ES (Space X Reports No Damage to Falcon 9 First Stage After Landing, 2016, Air Force assess more landing pads, Dragon processing at LZ-1, 2017, Blue Origin announces the first successful landing of a "reusable" rocket, 2015, Rocket and space developments: LV "ROSSIYANKA", 2012, United Nations Office for Outer Space Affairs, 2010);

– aerodynamic maneuver (aircraft scheme) using a winged scheme and landing in the launch area or a dedicated airfield (Kuznetsov and Ukraintsev 2016).

The aerodynamic maneuver scheme (aircraft scheme) was implemented in the Space Shuttle, Buran, X-37B projects.

In (Zharikov and Trushlyakov 2019), it was proposed to consider the project of equipping launch vehicle stages with autonomous onboard controlled descent systems (AODS) (Fig. 1), which will allow:

a) use a significantly lower IA of the expended booster stage of the LV;

b) completely exclude liquid residues of RPC in the ES fuel system;

c) implement the removal of the ES of the upper stages of the launch vehicle from the critical areas of the near-Earth outer space.

At the same time, in order to bring the ES to a predetermined point of impact in the selected impact area, the energy resources contained in the propellant components, as well as the residues of the compressed gas of the pressurization system of the ES fuel tanks, are used in full.

To study the possibility of removal the spent stage to a given aiming point, it is necessary to study the mechanisms for extracting guaranteed fuel reserves

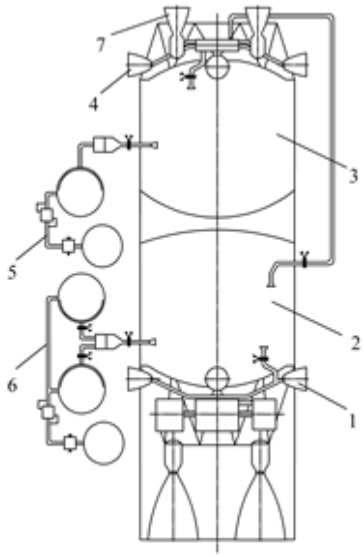

Fig. 1. AODS variant: 1 – gas-jet system nozzles for dumping a vapor-gas mixture of fuel from tank 2; 4 - gas-jet system nozzles for dumping a vapor-gas mixture of oxidizer; 5 - a system for HC for evaporation of oxidizer residues in tank 3; 6-a system for obtaining HC for evaporation fuel residues in tank 2; 7 - combustion chambers of a gas rocket engine.

for its subsequent processing and use in adjusting the spent stage-controlled flight trajectory. This concept as a scientific hypothesis is the main task of the study, the results of which are presented in this article.

The first part of the section deals with the physical modeling of the process of generating a guaranteed fuel supply in the tanks of ES of LV.

The second part of the section deals with mathematical modeling of the fuel evaporation process.

2. EXPERIMENTAL STUDIES ON THE EXTRACTION OF GUARANTEED RESERVE OF FUEL IN EXPENDED STAGE TANKS

An experimental stand was developed to study the processes of extraction of GRF, including the evaporation of liquid from a container at atmospheric pressure.

Scientific tasks to be solved during experiments:

a) Obtaining experimental dependencies on the change in the evaporation rate of the model fluid in the EMS at constant parameters of the supplied HC (temperature, mass-second flow, pressure in the volume of the EMS) and different angles of input of the HC relative to the longitudinal axis (0° and 30 °);

b) Conducting a comparative analysis of the results of mathematical modeling on the basis of two types of models (according to the 1st law of thermodynamics, according to the Navier-Stokes equations);

Fig. 2. Experimental model setup.

c) Conducting a comparative analysis of the results of mathematical and physical modeling.

Experimental studies were carried out on the created experimental model installation (Fig. 2), the geometric dimensions of which, as well as the (HC) parameter, are determined on the basis of similarity theory using similarity criteria, such as Nusselt, Reynolds and Prandtl (Suimenbayev *et al.* 2019a).

To increase the degree of result generality without losing the information contained in it, the fundamental features of technical means were applied. Based on the theory of dimensions and the theory of similarity, the formulation and task of the experiment is simplified and facilitated. At the same time, there is no need to study the functional relationships between the whole complexes of quantities that determine this phenomenon, as well as the need to study the influence of each factor on the process separately, which makes it possible to disseminate the results of individual studies on similar systems.

2.1 Program and Methodology of Experimental Research

The experimental program includes obtaining the following information:

- Influence of the angle of HC input on the parameters of the evaporation process,

- The effect of the mass second flow rate of HC on the parameters of the evaporation process,

- The effect of measuring the HC temperature on the parameters of the evaporation process.

The measured parameters include temperatures at the level of the installation of a bath with a model liquid, model liquid, heat carrier inside the experimental model setup, heat carrier at the entrance to the experimental model setup, the mass of the evaporating model liquid (initial and final).

As parameters of the process of evaporation of the model liquid in the experimental model setup, the pressure inside the experimental model setup during the experiment was taken to be 1 atm. and evaporation time 600 s.

The parameters of the supplied heat carrier include purified and dehumidified air with a moisture content of 5%, temperature 100 °C, mass-second flow rate 200 l/min; the angle of entry is 0°, 30° from the vertical axis, and the distance from the point of entry of the heat carrier to the mirror of the model liquid is approximately 485 mm.

The parameters of the model liquid include an initial temperature of 15.5 °C, an initial mass of 40 g; evaporation surface diameter (76mm) and distilled water for liquid type.

Limitations and assumptions adopted in the conduct of experimental studies:

a) Only the convective effect of the HC flux on the evaporated model fluid shall be considered, without chemical interaction.

b) The temperature and flow rate of the HC on the surface of the model fluid are determined from the conditions of the similarity theory.

c) The temperature of the model fluid throughout the volume is taken to be averaged.

d) The model fluid shall be considered without hesitation of the free surface.

e) There are no heat fluxes in the EMS between the model fluid and the EMS wall, since the model fluid is located in a bath that is isolated from the walls of the EMS.

The scheme of the experimental stand is presented in Fig. 3 (Trushlyakov *et al*. 2019).

2.2 Sequence of the Experiment

Before the series of experiments begins, all valves (3) are in the closed position. The compressor (1) is turned on and the air begins to flow into the pressure accumulator (PA) (2), after reaching the set pressure in the pressure accumulator, the compressor automatically shuts down. After that, all valves are opened except for the valve located in front of the entrance to the EMS (25). Compressed air is passed

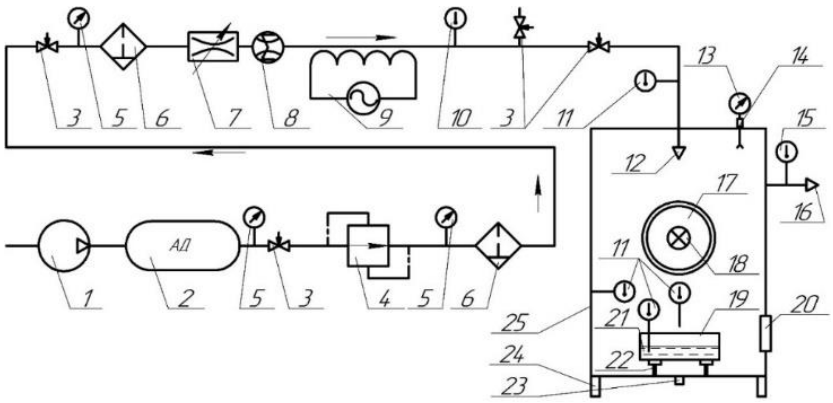

1 – Compressor; 2 – pressure accumulator; 3 – valve; 4 – gearbox; 5 – analog pressure sensor; 6 – filter- dehumidifier; 7 – adjustable throttle; 8 – flow sensor; 9 – electric heater; 10 – temperature control sensor HC at the outlet of the electric heater; 11 – mobile temperature sensors (thermocouple); 12 – fitting of the HC input into the EMS (replaceable nozzles with different cross-section and angle of inclination); 13 – digital pressure sensor; 14 – cooler for pressure sensor; 15 – temperature sensor; 16 – connection of the output of the HC from the EMS; 17 – viewing window; 18 – LED lamp; 19 – tank for model fluid; 20 – safety membrane; 21 – model liquid (distilled water); 22 – heat-insulating legs of tank 19; 23 – drain fitting; 24 – EMS support legs; 25 – EMS

Fig. 3. Scheme of the experimental stand.

through the gearbox (4) and at the outlet of the gearbox the necessary pressure in the line is set to ensure a constant rate of HC supply during the experiment. Next, the HC passes through the filter-dehumidifier (6), which consists of two filters of saw-moisture separators and a filter-regulator of pressure FESTO LFX-D, where it is pre-cleaned and dried. After the HC passes through the filter-dehumidifier of fine cleaning and enters the adjustable *throttle* (7), which allows to adjust the flow rate of the HC, the flow rate itself (in our case, 200 l / m) is controlled using a flow sensor (8). Next, the HC passes through the electric heater (9) and heated to 105 ° C, the temperature of the HC at the outlet of the electric heater is controlled by a temperature sensor (10), the measurement results are transmitted in real time to the control unit of the electric heater, which, based on the results obtained, turns the electric heater on or off. The heated HC is discharged into the atmosphere through the valve (3) after leaving the electric heater (9), this is done to achieve the necessary initial properties of the HC (temperature, flow) before the start of a series of experiments.

After reaching the HC at the outlet of the electric heater of the set temperature in the EMS (25), the model fluid (21) is placed with a given mass and temperature in the container for the model fluid (19). The container (19) through the heat-insulating legs (22) is located at the bottom of the EMS (25). The mass of the model fluid (21) is determined using laboratory balances installed outside the EMS.

The angle of injection of the HC in the EMS (25) is set before the start of the experiment, by installing a nozzle with a certain angle of inclination on the fitting (12).

After installing the model fluid in the EMS, the EMS cover is hermetically closed. It opens valve (3) located at the input to the EMS, and valve (3) located after the electric heater (9) closes and the HC begins to enter the EMS (25) through the input connector (12) HC in the EMS. Temperature sensors (11) in real time and throughout the experiment record and transmit through MIT-12 to a personal computer the temperature of the HC at the input to the EMS (25), the wall temperature of the EMS (25), the temperature in the model fluid (21), while the temperature sensor does not touch the walls of the container (19) and the temperature of the HC above the surface of the model fluid (21).

The pressure sensor (13) shows the pressure values inside the EMS (25), and the cooler (14) is used to prevent heating of the digital pressure sensor (13). Due to the fact that the HC is freely removed from the EMS (25) through the fitting (16), the pressure inside the EMS remains constant and equal to 1 atm. The temperature sensor (15) measures the temperature of the HC at the outlet of the EMS (25).

At the moment of HC supply to the EMS, a stopwatch is turned on to record the time of the experiment, when reaching 600 s, the experiment stops, the valve (3) at the entrance to the EMS (25) closes, and the valve (3) located after the electric heater (9) opens and the HC is discharged into the atmosphere. After the cap of the EMS (25), the container (19) with the model fluid (21) is removed and weighed to determine the mass of the evaporated model fluid.

Visualization of the liquid evaporation process is carried out through inspection windows (17).

2.3 Results of the Experiments

Based on the results of the experiments, a database of experimental studies was obtained, which includes changes in the mass of the liquid (water), the temperature of the liquid, the gas in the process of evaporation.

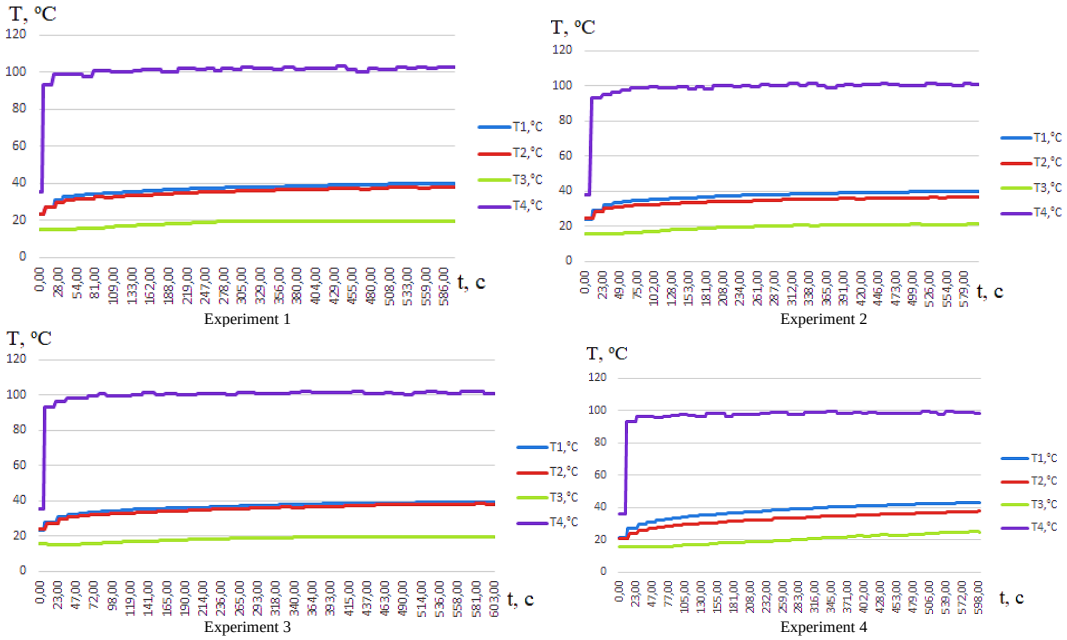

T1 - is the temperature of HC above the tank with a model liquid; T2 - is the temperature of the wall of the EMS; T3 - is the temperature of the model liquid; T4 - is the temperature of HC at the entrance to the EMS

Fig. 4. Temperature change over time in experiments on evaporation of a model liquid into an EMS with an input angle of HC into an EMS of 0° (Experiments 1,2,3) and 30° (Experiments 4).

The results of the conducted physical experiments of evaporation of a model liquid in an EMS with an input angle of HC into an EMS of 0 ° and 30° are shown in Fig. 4.

According to the results of the experiments, the following masses of the evaporated model liquid were obtained:

Experiment №1 – 5.2 g.

Experiment №2 – 5.1 g.

Experiment №3 – 5.4 g.

Experiment №4 – 1.5 g.

According to the results of the physical experiment, on average, for 600 seconds, at an input angle of 0 ° HC in the EMS, 5.2 g evaporates from 40 g of the initial mass of the model fluid, while the nature of the temperature change depending on time is the same in all experiments, and their values are identical taking into account the error of measuring instruments.

According to the results of the physical experiment, on average, over 600 seconds, at an input angle of 30° HC in the EMS, 1.5 g evaporates from 40 grams of the initial mass of the model fluid, while the nature of the temperature change depending on time is the same, and their values are identical taking into account the error of the measuring instruments (Suimenbayev *et al.* 2019).

With an injection angle of HC in the EMS of 0 ° and the same energy costs, the average mass of the evaporated model fluid is 3.5 times greater than at an input angle of 30 °. This is due to energy losses, which is clearly visible in the comparative graph of the change in the temperature of the HC at the outlet of the EMS at different angles of input of the HC, the temperature of the HC, the mass second flow rate of the HC, evaporation rate, etc. (Fig. 5).

3. COMPARATIVE ANALYSIS OF EXPERIMENTAL AND THEORETICAL STUDIES

3.1 Analysis of the Results of Modeling of Liquid Evaporation Processes Based on the Navier-Stokes Equations

The parameters characterizing the evaporation process include 6 values: the mass rate of evaporation, including under various mechanisms of vaporization (evaporation from the surface and bubble boiling, and film boiling is not considered in this article), saturation temperature, gas temperature in the tank, density, pressure, flow rate of the vapor-gas mixture from the container. Part of the values is determined as a result of the integration of equations (two temperatures, pressure, density), and such parameters as the mass rate of evaporation, the rate of outflow from the tank through the hole (nozzle) are determined on the basis of calculation formulas using correction coefficients.

In the numerical solution of the system of Navier-Stokes equations, a number of assumptions are provided, which are due to the specifics of the problems being solved, using numerical methods (Kuznetsov and Ukraintsev 2016), for example:

– introduction of the turbulence model, in particular, for modeling the boiling process in a closed volume, the standard k-ε turbulence model (k is the kinetic energy of turbulence, ε is the rate of viscous energy dissipation (dissipation of kinetic energy into

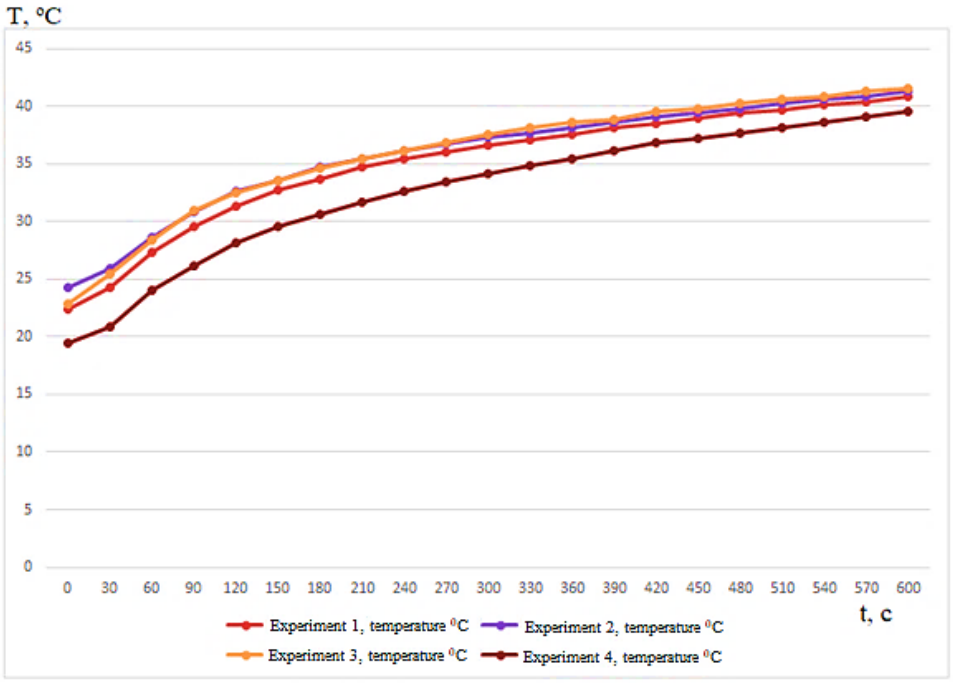

Fig. 5. Change in the temperature of the HC at the outlet of the EMS by time.

thermal energy) of turbulence) is recommended in ANSYS)

– two concepts of generation of turbulence P and dissipation of ε large vortices into smaller ones are introduced, which leads to a decrease in turbulence, which is similar to the values

– Based on the calibration of constants for this model, made on the basis of experimental data for jet streams, their values (depending on $C_2 = C_1 - \frac{k^2}{\sigma_\varepsilon \sqrt{C_\mu}}$) are selected, which are equal;

$C_2 = 1.92; C_1 = 1.44; \sigma_\varepsilon = 1.3; C_\mu = 0.09; \sigma_k = 1$

- The equation has a singularity (the solution tends to infinity and there is no exact solution). The dissipative term in the equation for ε will tend to infinity at k → 0; in addition, at y → 0, ε → 0 (assumptions and restrictions for the Navier-Stokes equations) and the value of turbulent viscosity becomes uncertain.

In the software product ANSYS Fluent (Odintsov 2009) for the process of vaporization and heat exchange, the equations of conservation of mass, momentum and energy equations are solved. The basic equation of heat transfer energy according to Navier-Stokes is of the form:

$$\frac{\partial}{\partial t}\left(\rho\left(h-\frac{p}{\rho}+\frac{v^2}{2}\right)\right)+\nabla\cdot(\vec{v}\,(\rho\left(h-\frac{p}{\rho}+\frac{v^2}{2}\right)+p))=\nabla\cdot\left(\lambda\nabla T-\Sigma_j h_j\vec{J}_j+\left(\tau_{eff}*\vec{v}\right)\right)+S_h; \quad (1)$$

where: ρ, p, T- density, pressure and temperature, respectively, λ -thermal conductivity, S_h- the amount of heat including heat from chemical reactions, or other sources of heat, $\vec{J}$ - diffuse particle flow, h_j- particle enthalpy, $\vec{v}$ - velocity vector, τ_{eff} - stress deviation tensor, representing viscous heating.

The equation for conservation of mass is:

$$\frac{\partial\rho}{\partial t}+\nabla\cdot\left(\rho\vec{v}\right)=S_m \quad (2)$$

where: S_m is the mass added by vaporization of the liquid during heat exchange.

The conservation equations are:

$$\frac{\partial}{\partial t}\left(\rho\vec{v}\right)+\nabla\cdot(\rho\vec{v}\,\vec{v})=-\nabla p+\nabla\cdot\bar{\tau}+\rho\vec{g} \quad (3)$$

Where $\bar{\tau}$ - tensor of stresses, $\rho\vec{g}$ - gravitational force.

The mass rate of evaporation from the surface is determined by the formula:

$$\frac{\partial}{\partial t}(\alpha\rho_v)+\nabla\cdot(\alpha\rho_v\vec{V}_v)=\dot{m}_{l-v}-\dot{m}_{v-l}, \quad (4)$$

where: α, ρ_v,- volume fraction of steam, vapor density; $\vec{V}_v$ - Steam phase velocity, $\dot{m}_{l-v}, \dot{m}_{v-l}$ - mass rates of evaporation, condensation.

At the temperature of the liquid greater than the saturation temperature, the evaporation process occurs, which is determined by the Hertz-Knudsen formula (Shalay 2000):

$$\dot{m_{l-v}} = coeff * \alpha_l * \rho_l * \left(\frac{T^*-T_{sat}}{T_{sat}}\right) = \beta\sqrt{\frac{M}{2\pi R T_{sat}}}L\left(\frac{\rho_v\rho_l}{\rho_l-\rho_v}\right)*\left(\frac{T^*-T_{sat}^1}{T_{sat}}\right), \quad (5)$$

where: M- molar mass of the liquid, R- gas constant, ρ_l - density of the liquid phase, L- heat of vaporization, T^*- steam temperature near the liquid in the container, T_{sat} - saturation temperature of water at pressure in the container, *coeff*- coefficient, inverse of the relaxation time.

3.2 Equations Based on the First Law of Thermodynamics

The system of equations based on the first law of thermodynamics is of the form (Baranov *et al.* 2015; Avdoshkin *et al.* 2016; Karrask *et al.* 2018):

$$\begin{cases} \frac{dp}{dt} = \frac{k-1}{V}(Q_\Sigma + i_{ev}\dot{m}_{ev} - i_{out}\dot{m}_{out}), \\ \frac{d\rho}{dt} = \frac{1}{V}(\dot{m}_{ev} - \dot{m}_{out}), \\ \frac{dT_{mix}}{dt} = \frac{q_{rad}^{w-mix} + q_{con}^{w-mix}}{c_{mix}m_{mix}}, \\ \frac{dT_w}{dt} = \frac{q_\Sigma - q_{rad}^{w-lox} - q_{con}^{w-lox} - q_{rad}^{w}}{c_w m_w}, \\ \frac{dT_{lox}}{dt} = \frac{q_{rad}^{w-lox} + q_{con}^{w-lox} - q_{ev}}{c_{lox}m_{lox}} \end{cases} \quad (6)$$

1 - pressure change, 2 - gas density change, 3 - gas temperature, 4 - wall temperature, 5 - liquid temperature

Where $p, \rho, V, T_w, T_{lox}, T_{mix}$ are the pressure in the tank, the density, the free volume of the container, the wall temperature, the temperature of the liquid, the temperature in the container respectively, $\dot{m}_{ev}, \dot{m}_{out}$ are the mass flow of the evaporated liquid, at the outlet of the container, respectively; i_{ev} – enthalpy of the evaporated liquid, q_{ev} – heat of evaporation of the liquid, c_w, c_{lox},, m_w, m_{lox} – heat capacity of the container wall, liquid, as well as the mass of the container wall, liquid, respectively, the external heat flow q_Σ.

The mass rate of evaporation $\dot{m}_{ev}$ is defined as the sum of evaporation from the surface of a liquid (Hertz-Knudsen formula) and boiling of a liquid (according to law 1 of thermodynamics) according to the formula:

$$\dot{m}_{ev} = \dot{m}_{int} + \dot{m}_{boil} = \beta\sqrt{\frac{M}{2\pi RT_{sat}}}L\left(\frac{\rho_v\rho_l}{\rho_l - \rho_v}\right) * \left(\frac{T^* - T_{sat}^1}{T_{sat}}\right) + \frac{q_{rad}^{w-lox} + q_{con}^{w-lox}}{Q_{ev}}, \quad (7)$$

where: $\dot{m}_{int}, \dot{m}_{boil}$ are the mass evaporation rates of the liquid from the surface and as a result of boiling, respectively.

The mass flow through the hole $\dot{m}_{out}$ is determined by the formula:

$$\dot{m}_{out} = \mu m F_{out}\phi\frac{p(t)}{\sqrt{T(t)}} \quad (8)$$

where: μ- flow coefficient, F_{out}- the area of the passage section of the outlet hole, m^2, $p(t)$- pressure in the tank, Pa; $T(t)$- temperature in the tank, K.

ϕ- A coefficient determined by the formula:

$$\phi = \begin{cases} 1, & b \le b_{cr} \\ \sqrt{b^{2/k} - b^{k+1/k}}, & b > b_{cr} \end{cases}, b = \frac{p_h}{p_b}, \quad (9)$$

the index h indicates the greater of the pressures (inside the tank or outside it), b - less, for k = 1.4, the critical value of the pressure ratio b_{cr} = 0.528.

m - Gas-dynamic function:

$$m = \begin{cases} \sqrt{2k/(k-1)R}, & b \le b_{cr} \\ \sqrt{k/R((2/k+1))^{(k+1)/(k-1)}}, & b > b_{cr} \end{cases} \quad (10)$$

here R is the specific gas constant.

$q_{rad}^{mix-lox}$ - radiant component from the combined-cycle mixture to the liquid:

$$q_{rad}^{w-lox} = \sigma\varepsilon_w F_w\left(\left(\frac{T_w(t)}{100}\right)^4 - \left(\frac{T_{lox}(t)}{100}\right)^4\right) \quad (11)$$

here $\sigma, \varepsilon_w, F_w, T_w(t), T_{lox}(t)$ is the Stefan-Boltzmann constant, the degree of blackness of the wall, the area in contact with the liquid, the walls of the container, the wall temperature, the temperature of the liquid, respectively.

$q_{con}^{mix-lox}$ - convective component from the combined-cycle mixture to the liquid.

$$q_{con}^{w-lox} = \alpha_w F_w(T_w(t) - T_{lox}(t)) \quad (12)$$

Here α_w is the heat transfer coefficient from the combined-cycle mixture to the liquid.

3.3 Analysis of the Results Modeling of the Evaporation Process Based on Two Mathematical Models

When conducting numerical modeling, the initial data were used:

Boundary conditions: experimental capacity in the form of a cylinder with a size of 720 * 260 * 260 mm. Outlet with a diameter of 20 mm.

Initial conditions: heating the liquid to the boiling point;

Thermal impact: heat flux density of 15000 W/m2 (which corresponds to heat flux at an altitude of 35 km).

Selection of heat transfer α_w coefficient, accommodation coefficient β from the conditions:

– the coefficient of heat transfer α_w during boiling water can vary in the range from 2000 to 40000 W/m^{2}K.

– the accommodation coefficient β (Suimenbayev *et al.* 2019b) was determined experimentally during the evaporation of distilled water from 313 K to 363 K. It is concluded that the accommodation coefficient β

increases with increasing temperature and for this temperature range (313 K- 363 K) varies from 0.00013 to 0.00024 kg / m^2s. At this stage of calculations for the boiling process, the accommodation coefficient was chosen to be equal to 0.0003 kg / m^2s.

In the future, it is planned to conduct experimental studies in particular to determine the coefficient of accommodation of water at boiling.

- When calculating in ANSYS, the *coeff* coefficient depends on the value of the accommodation coefficient β, which is determined experimentally. At this stage, the *coeff* coefficient, according to the selected value of the accommodation coefficient, is 0.03 1 / s. In the following works, an experimental refinement of these coefficients is planned.

d) in the comparative analysis of the parameters of the fluid evaporation processes obtained on the basis of the numerical solution of the Navier-Stokes equations and the first law of thermodynamics, the average values of the parameters of the solution parameters of the Navier-Stokes equations are used.

e) in equations (6) – (12), when modeling according to the 1st law of thermodynamics, only the bubble boiling regime of the liquid and evaporation from the surface is considered.

Below in Figs 6-12 present the results of calculations of the evaporation process based on two methods.

According to ANSYS calculations, the density of the gas decreases to a value equal to the vapor density of steam (the density of water vapor is 0.55 kg / m^3). According to the first law of thermodynamics, the density of the gas in the tank decreases slightly (by 0.01 kg / m^3). The difference in calculations is 34%. To reduce the deviation, the value of the accommodation coefficient can be reduced, but at the same time the differences in the values of other parameters (pressure, flow rate, mass evaporation rate, thrust) will be increased.

The difference in calculations for the 2 methods is less than 2%". The variable is the pressure in the tank. An increase in pressure in the ANSYS calculation of up to 30 seconds is associated with an increase in the temperature in the tank (Fig. 6) and the mass flow rate at the outlet of the hole. The data correspond to the experimental stand. A further decrease in pressure is associated with a similar decrease in the mass flow rate atthe outlet of the hole.

As follows from Fig. 8, the gas temperature in the tank according to method 1 changes more slowly in comparison with method 2, while by the end of the calculation the gas temperature in the tank reaches a higher value (377.3 K according to method 1, 375.3. K according to method 2).

ANSYS takes into account the laws of the kinetic theory of gas, which is why the output to the "working process" of the outflow does not occur immediately.

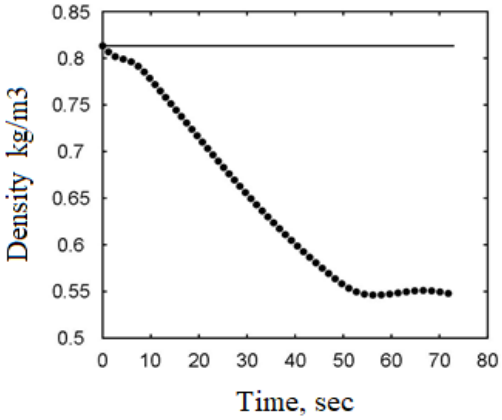

Fig. 6. Graph of density change in container (dotted line – ANSYS calculation, solid line – calculation according to the 1st law of thermodynamics).

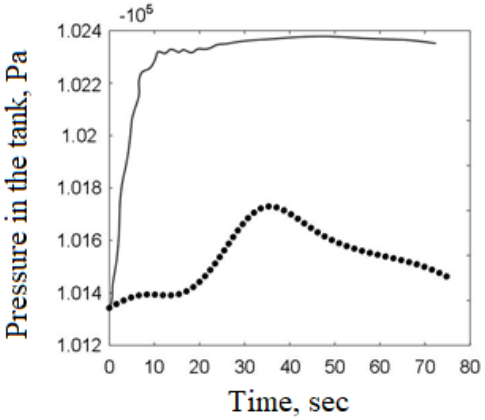

Fig. 7. Graph of pressure change in container (dotted line – ANSYS calculation, solid line – calculation according to the 1st law of thermodynamics).

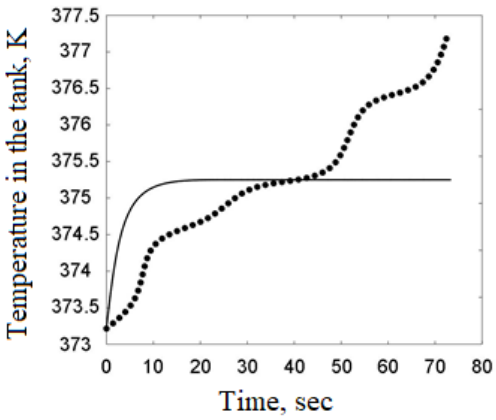

Fig. 8. Graph of gas temperature change in capacitance (dotted line – ANSYS calculation, solid line – calculation according to 1 law of thermodynamics).

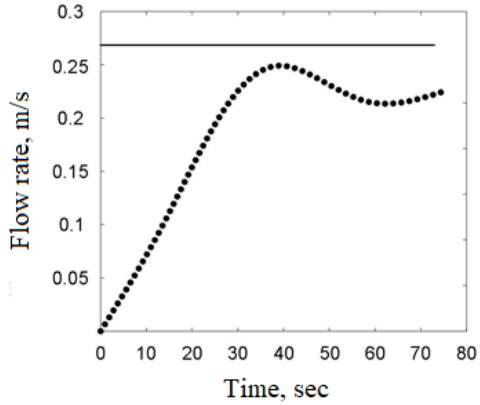

Fig. 9. Graph of the change in the flow rate from the hole ('dotted line' – ANSYS calculation, 'solid' line – calculation according to the 1st law of thermodynamics).

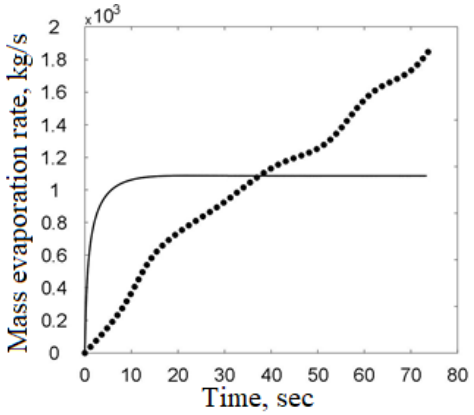

Fig. 10. Graph of the mass evaporation rate of the liquid ('dotted line' – ANSYS calculation, 'solid' line – calculation according to the 1st law of thermodynamics).

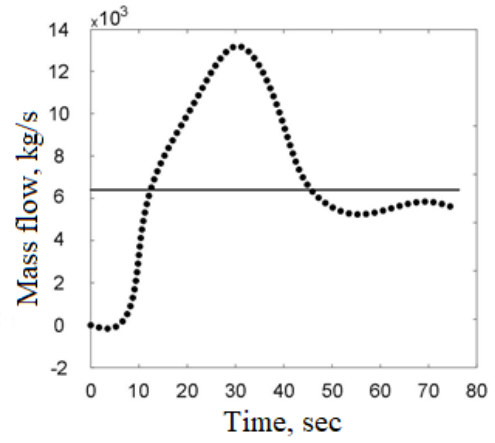

Fig. 11. Graph of change in mass gas flow at the output ('dotted line' – ANSYS calculation, 'solid' line – calculation according to the 1st law of thermodynamics).

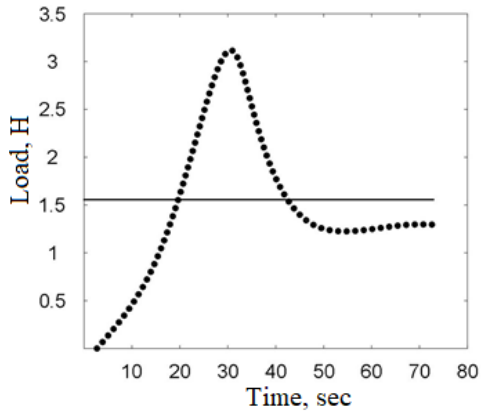

Fig. 12. Graph of the change in thrust when the combined-cycle mixture is discharged from the hole ('dotted line' – ANSYS calculation, 'solid' line – calculation according to the 1st law of thermodynamics).

As follows from Fig. 9 The difference in calculations for 2 methods is less than 13% after 30 seconds of calculation. According to the 1st law of thermodynamics, the calculation is carried out according to a concentrated model and from 1 second there is an exit to the "working process" of evaporation of water and gas outflow from the hole.

As follows from Fig. 10, the mass evaporation rate for the 2 methods varies similarly to the temperature in the tank (Fig. 11) . When calculating according to the 1st law of thermodynamics, the evaporation of the liquid occurs evenly during the entire calculation. The total amount of evaporated liquid according to the 1st method is 0.725 kg, according to the 2nd method is 0.75 kg. Deviation is 4%.

As follows from Fig. 11, after 40 seconds, the gas mass flow graphs have a smaller value difference (less than 14%). The mass flow rate of gas at the output in the ANSYS calculation at 30 seconds is associated with a similar increase in the pressure in the tank (Fig. 7).

The total amount of gas released from the tank for 72 seconds according to the 1st method is 0.52 kg, according to the 2nd method is 0.45 kg. Deviation is less than 10%.

As follows from Fig. 12, the change in thrust is similar to the change in the flow rate of the steam gases of the mixture from the hole (Fig. 11). The thrust pulse in method 1 (Fig. 12) is 0.1067 s, and in method 2 is 0.11 s. The difference in calculated thrust pulses is less than 3%.

Preliminary assessments are carried out using mathematical modeling in the ANSYS Fluent package divided into 3 stages:

(a) Modelling of velocity fields on the surface at different input angles of the vapor-gas mixture (VGM):

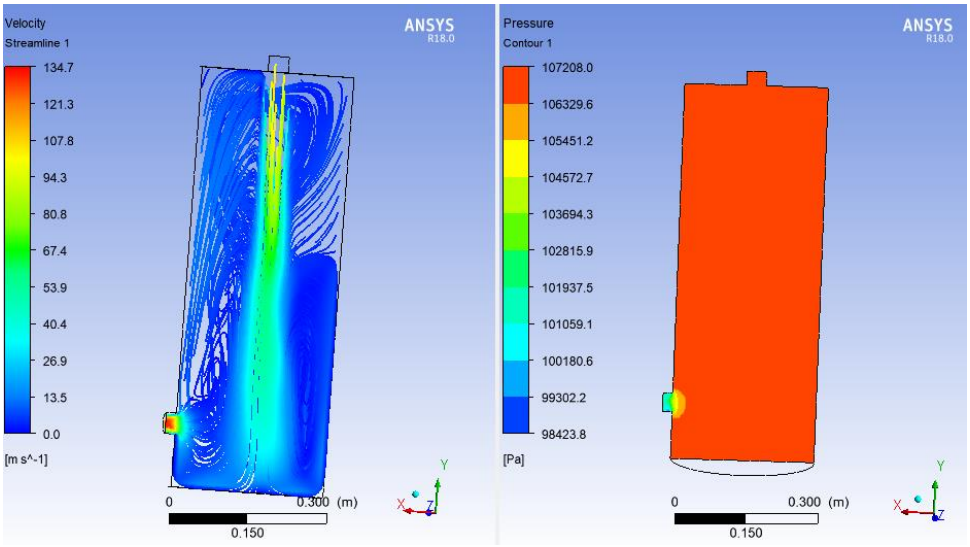

(a) (b)

Fig. 13. Input angle VGM 90°: a) VGM current line b) pressure in the chamber

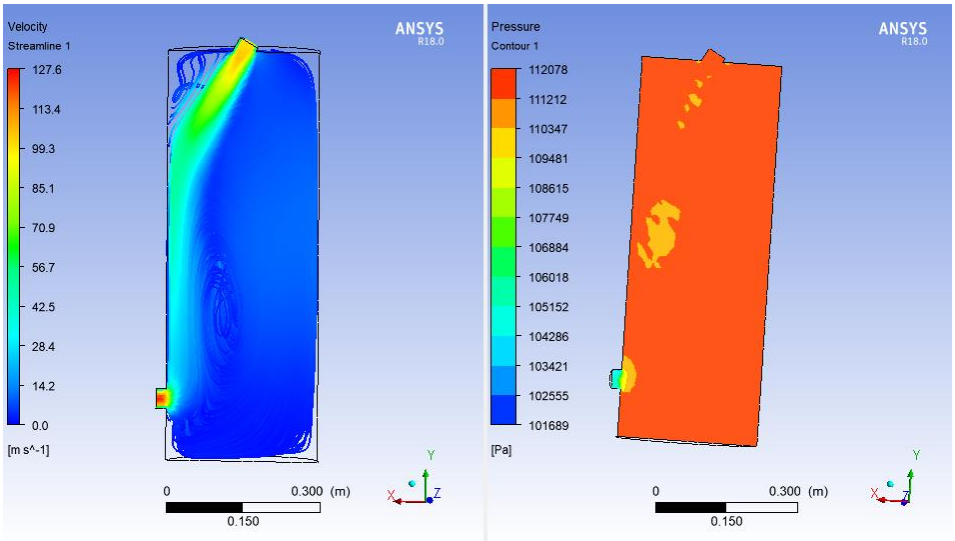

(a) (b)

Fig. 14. Input angle VGM 45°: (a) VGM current line (b) pressure in the chamber.

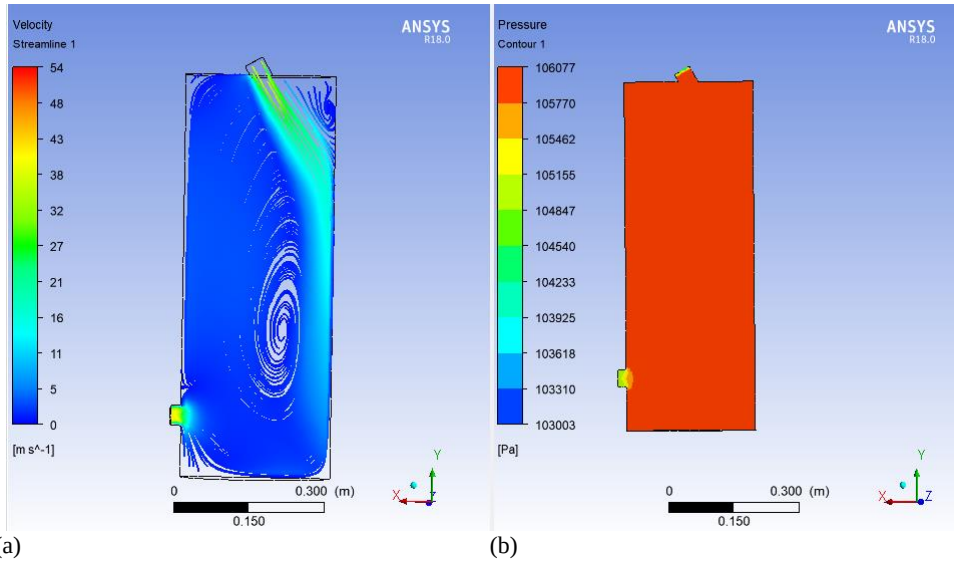

(a) (b)

Fig. 15. Input angle VGM 135°: a) VGM current line b) pressure in the chamber.

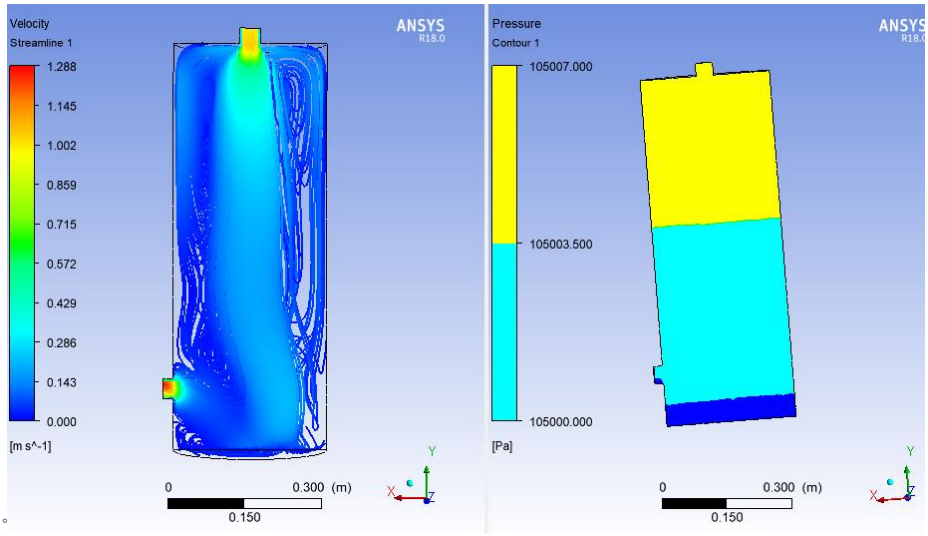

(a) (b)

Fig. 16. VGM injection rate is 1 m/s: (a) VGM current lines (b) chamber pressure.

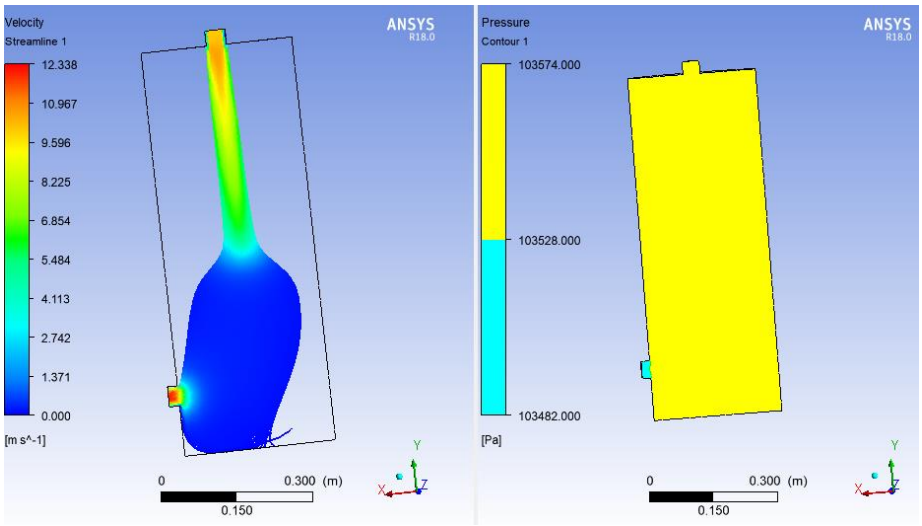

(a) (b)

Fig. 17. VGM injection rate is 10 m/s: (a) VGM current line (b) chamber pressure.

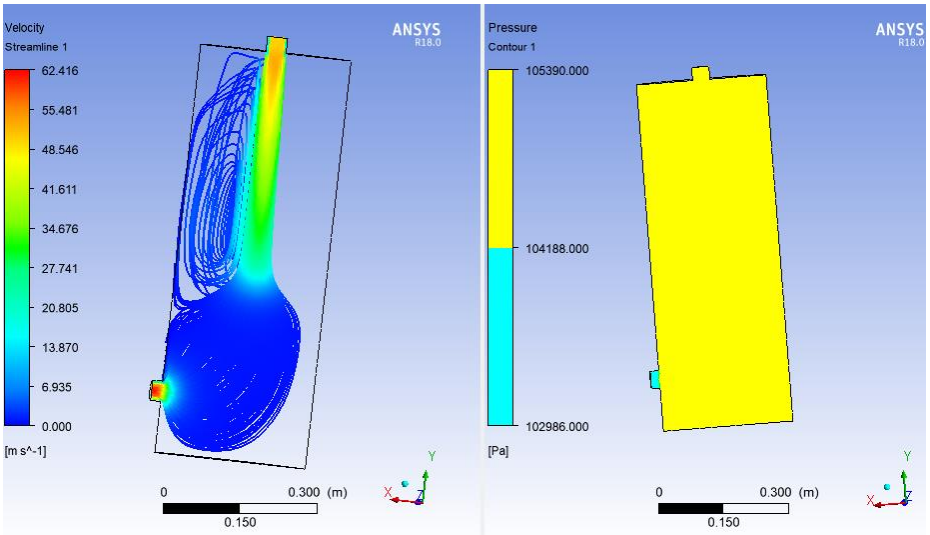

(a) (b)

Fig. 18. The VGM injection rate is 50 m/s: (a) VGM current line (b) chamber pressure.

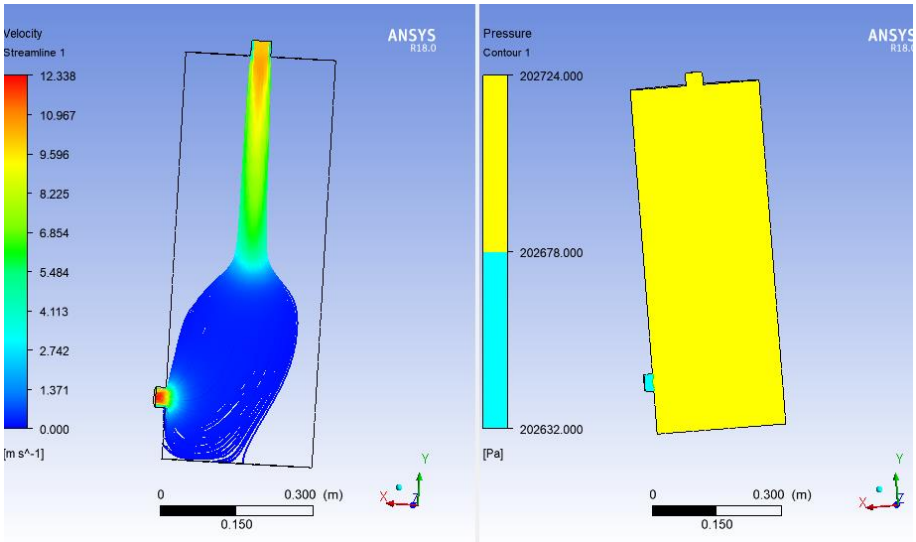

(a) (b)

Fig. 19. Pressure in the chamber is 2 atm.: (a) VGM current line (b) the pressure in the chamber

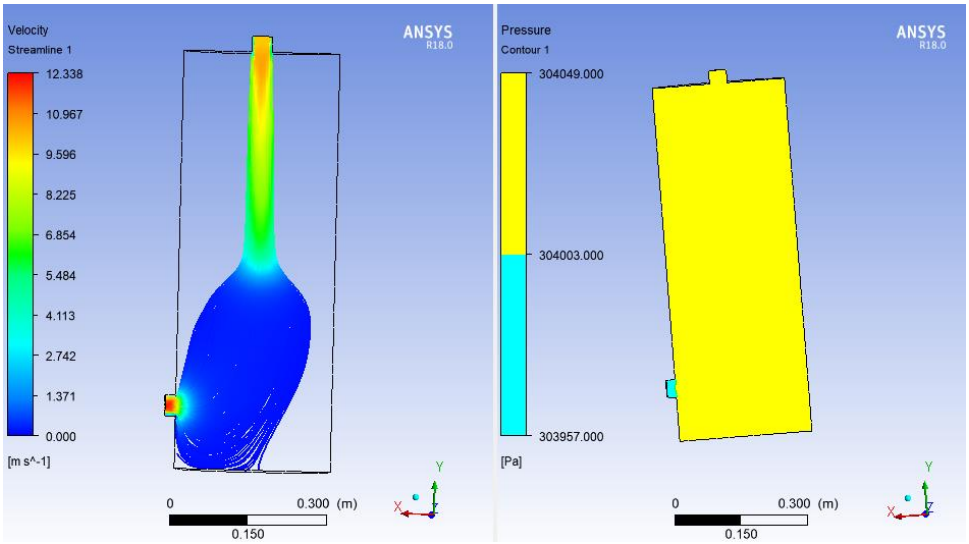

(a) (b)

Fig. 20. Pressure in the chamber is 2 atm.: (a) VGM current line (b) the pressure in the chamber.

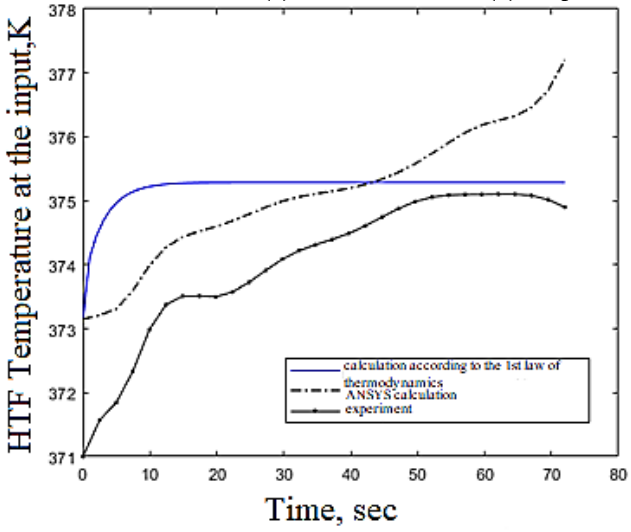

Fig. 21. Graph of comparison of the temperature of the HC at the input to the EMS for the estimated time.

The input speed of the vapor-gas mixture is 100 m/s. The diameters of the inlet and outlet of the chamber are 40 mm. The pressure in the chamber is 1 atm.

b) modeling of velocity fields on the surface at different input rates of the VGM:

The input speeds of the VGM are 1/10/50 m/s. The diameters of the inlet and outlet of the chamber are 40 mm. The pressure in the chamber is 1 atm. The injection angle of the VGM is 90 c) modeling of velocity fields on the surface at different pressures in the chamber:

The speed of input of the VGM is 10 m / s. The dia-

meters of the inlet and outlet of the chamber are 40 mm. The velocity fields on the surface at a pressure of 1 atm. are shown in Figs. 13-20.

3.4 Analysis of the Results of Mathematical and Physical Modeling

A comparison of the results of mathematical modeling and physical modeling is carried out. The calculated temperatures of the HC at the input to the EMS (according to the first law of thermodynamics and the Navier-Stokes equations) and the measured temperature of the HC at the entrance to the EMS during the conduct of experiments were compared (Fig. 21).

As follows from Fig. 21 The deviation of the experimental value of the temperature of the HC on the course from the calculated values is less than 10%. To reduce the deviation of the results of the calculation according to the Navier-Stokes equations from the experimental results, it is necessary to conduct additional experiments to determine the accommodation coefficient (Shalay 2000).

5. CONCLUSION

1. The first method, based on the Navier-Stokes equations and solved in ANSYS, has a number of assumptions, which leads to a simplification of the physical picture of the process;

2. The calculated deviations of 2 methods for the thrust impulse (less than 3%) have acceptable values, which allows the use of a method based on the 1st law of thermodynamics in engineering estimates;

3. Experimental studies are needed to obtain data on pressure, velocity, temperature, mass rate of evaporation to confirm the accommodation coefficient β, the evaporation frequency coefficient *coeff*, which is used in the ANSYS calculations, the boiling heat transfer coefficient α_w, the flow rate from the hole μ.

4. To carry out calculations using the ANSYS software package for the evaporation of other liquids (kerosene, liquid oxygen, liquefied methane), it is necessary to know the values of the accommodation coefficient calculations for liquid oxygen,

5. One of the advantages of using the method according to the 1st law of thermodynamics is the lack of determination of the accommodation coefficient, the coefficient of the inverse relaxation time.

When calculating the processes of evaporation of fuel components, oxygen, liquefied natural gas, kerosene when using a system of equations based on the first law of thermodynamics, the values of the heat transfer coefficients from the combined-cycle mixture α and β the accommodation coefficient, which are determined experimentally, are necessary.

The obtained results make it possible to use the residues of the guaranteed fuel reserve for the development of an autonomous onboard system for launching the spent part of promising launch vehicles, which will ensure:

a) fire and explosion safety of ES,

b) minimization of the ES fall area,

c) the ability to maneuver to change the location of the ES fall area.

ACKNOWLEDGEMENTS

The research was carried out with the support of the Science Committee of the Ministry of Education and Science of the Republic of Kazakhstan within the framework of grant No. AP09258759 "Development of a model of an information and forecast system for determining the launch and impact areas of ultralight launch vehicles, taking into account the requirements of environmental safety", will serve as the basis for the development of promising launch vehicles and will allow to work out the design parameters of the LV for the controlled descent of expended stages.

REFERENCES

Avdoshkin, V., V. N. F. Averkiev, A. A. Ardashov and others (2016). Problematic issues of the use of spacecraft launch routes and areas of fall of spacecraft separating parts: monograph; edited by A. S. Fadeeva, N. F. Averkieva. - St. Petersburg Russia: Military Space Academy named after A.F. Mozhaisky.

Baranov, D. A., N. Makarov Yu, V. I. Trushlyakov and T. Shatrov Ya (2015). The project of creating an autonomous on-board system for the introduction of spent stages of carrier rockets into specified areas. *Astronautics and rocket science* 50 (84), 76-82.

Blue Origin Makes Historic Reusable Rocket Landing in Epic Test Flight (2015). URL: https://www.space.com/31202-blue-origin-historic-private-rocket-landing.html

Karrask, V. K., N. A. Zharkova, V. N. Kamenshchikov, A. A. Latyshev, S. P. Pukhov, V. I. Potemkin and V. I. Talmazan (2018). Method for neutralizing fuel and oxidizer in the separating stages of a launch vehicle and a

device for its implementation. Patent No. RU2290352C2. Moscow, Russia.

Kuznetsov Yu, L. and D. S. Ukraintsev (2016) Analysis of the effect of the scheme of the flight stage with a rocket-dynamic rescue system on the energy characteristics of a medium-class two-stage launch vehicle. *Aircraft and Space Rocket Engineering* 15(1),73-80.

Odintsov, P. V. (2009). *Development of A Methodology for Selecting Design Parameters of On-Board Systems for Gasification of Liquid Fuel Residues of Missile Launch Vehicles.* Ph. D. Thesis, The Omsk State Technical University, Omsk, Russia.

Makeyev V. P. (2009) State Rocket Centre, "ROSSIYANKA LV" URL: https://iz.ru/838754/mikhail-kotov/nasha-korona-kak-otechestvennye-inzhenery-obognali-vremia.

Shalay, V. V. (2000). *Theoretical Foundations and Methodology of Processes of Thermal Decontamination of Fuel Residues in Separated Parts of Missiles*. Ph. D. thesis, The Omsk State Technical University, Omsk, Russia.

Shatrov, Y. T., D. A. Baranov, B. T. Suimenbayev and V. I. Trushlyakov (2016). Fire and explosion safety improvement during the launch vehicle worked-off stages with liquid propulsion engine operation. *Fire and Explosion Safety* 25(4), 30–42.

Space Debris Mitigation Guidelines of the Committee on the Peaceful Uses of Outer Space (2010). United Nations Office for Outer Space Affairs/ Vienna. URL: https://www.unoosa.org/documents/pdf/psa/bsti/COPUOS_SPACE_DEBRIS_MITIGATION_GUIDELINES.pdf

Space X Reports No Damage to Falcon 9 First Stage after Landing (2016). URL: https://spacenews.com/spacex-reports-no-damage-to-falcon-9-first-stage-after-landing/

Space X, Air Force assess more landing pads, Dragon processing at LZ-1 (2017). URL: https://www.nasaspaceflight.com/2017/01/spacex-air-force-landing-pads-dragon-lz-1/

Suimenbayev, B. T., V. I. Trushlyakov, G. T. Yermoldina, Zh. B. Suimenbayeva and A. M. Bapyshev (2019a). Business-process development of the information analytical Systems of the Baikonur cosmodrom and launch vehicle design for ecological safety Improving in the impact areas of the worked-off stages. Physical-Mathematical Series, 323(1), 5-–13. http://doi.org/10.32014/2019.2518-1726.1

Suimenbayev, B. T., V. I. Trushlyakov, G. T. Yermoldina, Zh. B. Suimenbayeva and A. M. Bapyshev (2019b). Problems of development, manufacturing and operation of rocket and space technology and training of engineering staff for the aerospace industry. In the Materials of the XIII All-Russian Scientific and Technical Conference Dedicated to the Memory of the Chief Designer "Flight" by A. S. Klinyshkov, Omsk, Russia.

Trushlyakov, V. I., B. T. Suymenbaev, V. A. Sevoyan, G. T. Ermoldina, Zh. B. Suymenbaeva and A. M. Bapyshev (2019). Methodology of experimental studies of obtaining steam-gas mixtures for controlling the movement of spent stages of launch vehicles during descent from the launch trajectories. In *IV International Scientific and Practical Conference "Computer Science and Applied Mathematics", dedicated to the 70th anniversary of Professors Biyarov T.N., Waldemar Vuytsik and 60 anniversary of Professor Amirgaliev E.N* Institute of information and computational technologies. Almaty, Kazakhstan.

Zharikov, K. I. and V. I. Trushlyakov (2019). Modeling the process of vapor–gas mixture outflow from the drainage manifold of the rocket-carrier stage. *Engineering Physics Journal* 92(3), 1-13.